



*Supplement of*

## **Impacts of elevated anthropogenic emissions on physicochemical characteristics of black-carbon-containing particles over the Tibetan Plateau**

**Jinbo Wang et al.**

*Correspondence to:* Jiaping Wang (wangjp@nju.edu.cn)

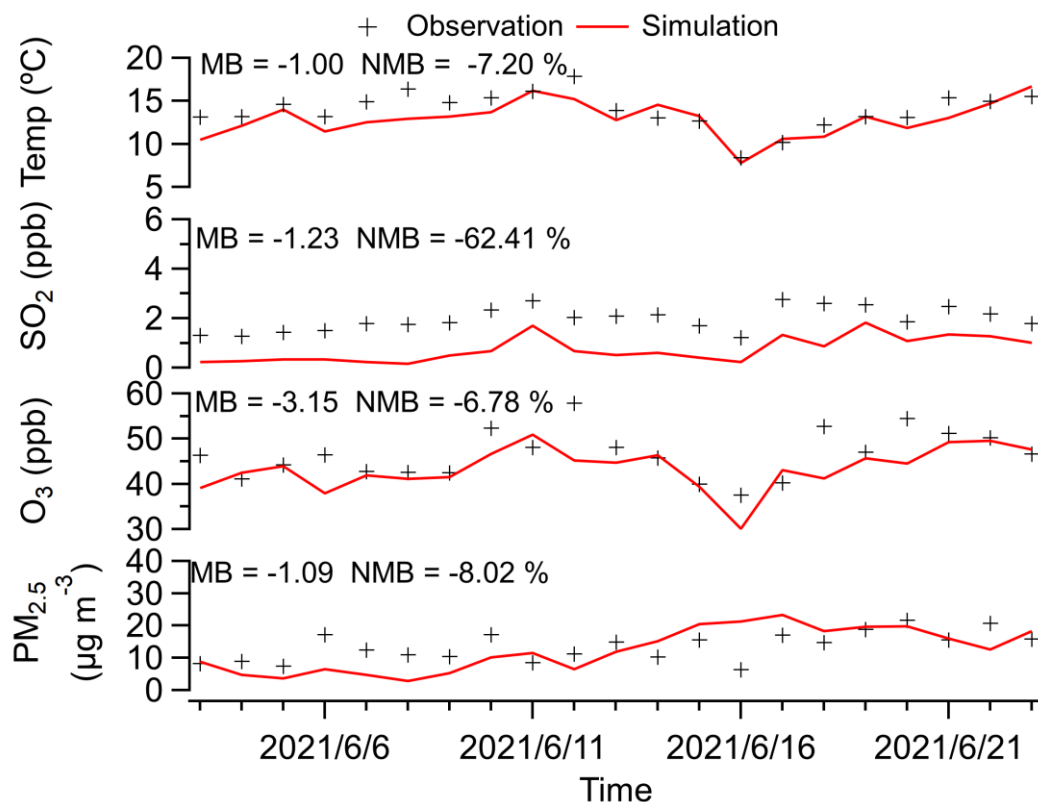
The copyright of individual parts of the supplement might differ from the article licence.

1 **S1 Model configuration**

2 **Table S1. WRF-Chem model configuration options and settings**

<b>Domain setting</b>	
Horizontal grid	160 × 180
Grid spacing	20 km × 20 km
Vertical layers	30 eta levels
<b>Configuration options</b>	
Long-wave radiation	RRTMG
Short-wave radiation	RRTMG
Cumulus parameterization	Grell–Deveny
Land-surface	Noah
Planetary boundary layer	YSU
Microphysics	Lin microphysics scheme
photolysis	Fast-J
Gas chemistry	CBMZ
Aerosol chemistry	MOSAIC

3

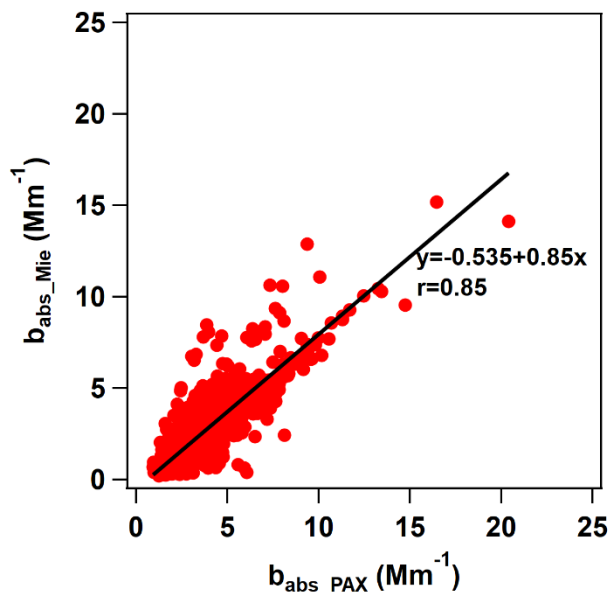


5

6 **Figure S1: The time series of the near-surface air temperature, sulfur dioxide (SO<sub>2</sub>), ozone (O<sub>3</sub>) and mass concentration of fine**  
 7 **particulate matter (PM<sub>2.5</sub>) in the Xihai and surrounding area. The line and marker represent the results of ambient measurement**  
 8 **and modelling respectively. The MB and NMB are mean bias and normalized mean bias of each parameter.**

9 In this study, the air temperature at 2 m were evaluated based on the measurement data from our measurement and publicly  
 10 available meteorological datasets of the University of Wyoming (<http://www.weather.uwyo.edu/surface/>). The air temperature  
 11 was pretty close between the modelling and measurement, and the mean bias was -1.00 °C. It was shown that the model had a  
 12 good performance in the simulation of meteorological fields.

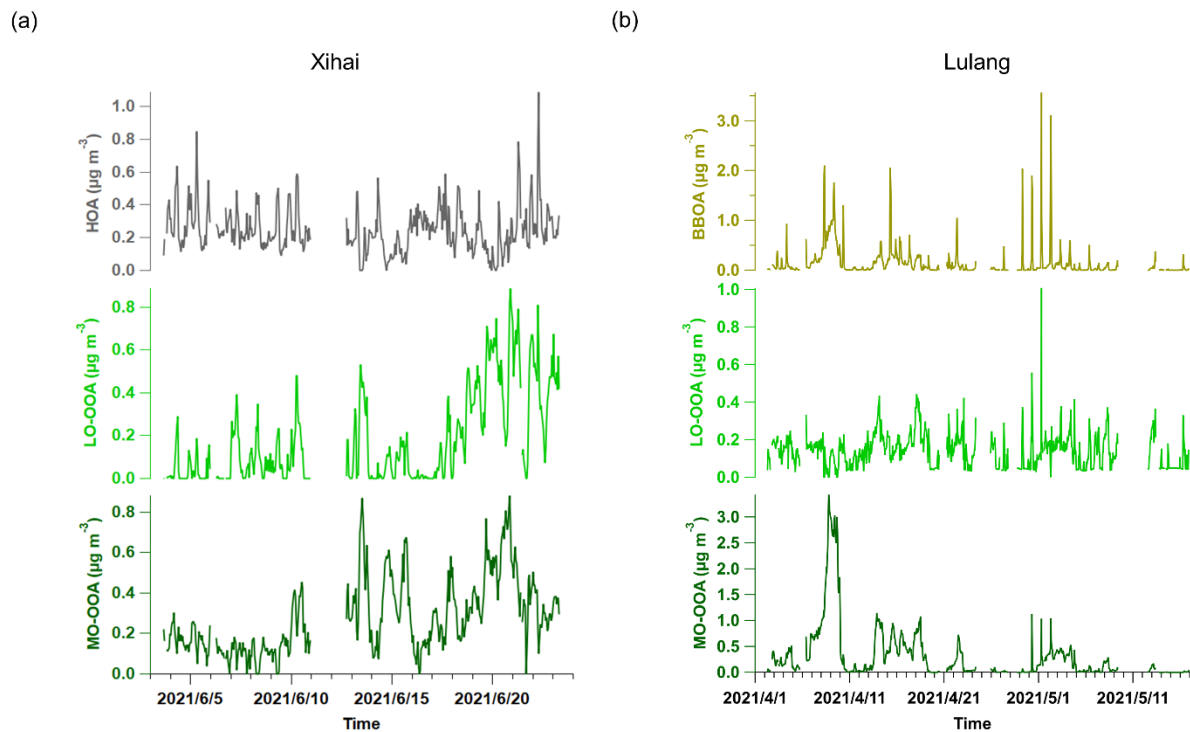
13 The air quality dataset at Xihai and the monitoring stations near to Xihai (<https://quotsoft.net/air/>) were used to evaluate  
 14 the WRF-Chem model in simulating the air pollution. There were overall good agreement and small bias between model-  
 15 simulated and observed concentration values of gaseous pollutant (SO<sub>2</sub>, O<sub>3</sub>) and particulate matter. The modelled SO<sub>2</sub>  
 16 concentration level is relatively low, however, it is not the pollutants of major concern in this study.



18

19 **Figure S2: The scatter plot, correlation coefficient and linear regression result of the aerosol light absorption coefficients ( $b_{\text{abs}}$ )**  
 20 **at 550 nm wavelength from different methods. The value of  $x$ -axis is the  $b_{\text{abs}}$  measured by the photoacoustic extinctions (PAX),**  
 21 **and the value of  $y$ -axis is the  $b_{\text{abs}}$  calculated by Mie theory. The  $b_{\text{abs\_PAX}}$  was converted from 870 nm to 550 nm wavelength based on**  
 22 **an rBC absorption Ångström Exponent of 1.0 (Moosmüller et al., 2011). The  $r$  is Pearson correlation coefficient in the plot.**

23 The more aged black carbon (BC)-containing particles ( $\text{PM}_{\text{BC}}$ ) can transport from other regions to Tibet Plateau (Chen et  
 24 al., 2019). The long-range transport reduces differences in the amount of coating between different BC particles (Cappa et al.,  
 25 2019). So, it is reasonable that using Mie theory (Mätzler., 2002) to calculate optical parameters of  $\text{PM}_{\text{BC}}$  in Xihai and Lulang.  
 26 Moreover, the  $b_{\text{abs}}$  acquired by the Mie theoretical calculations and PAX measurement is very close, and has higher correlation  
 27 ( $r=0.85$ ).

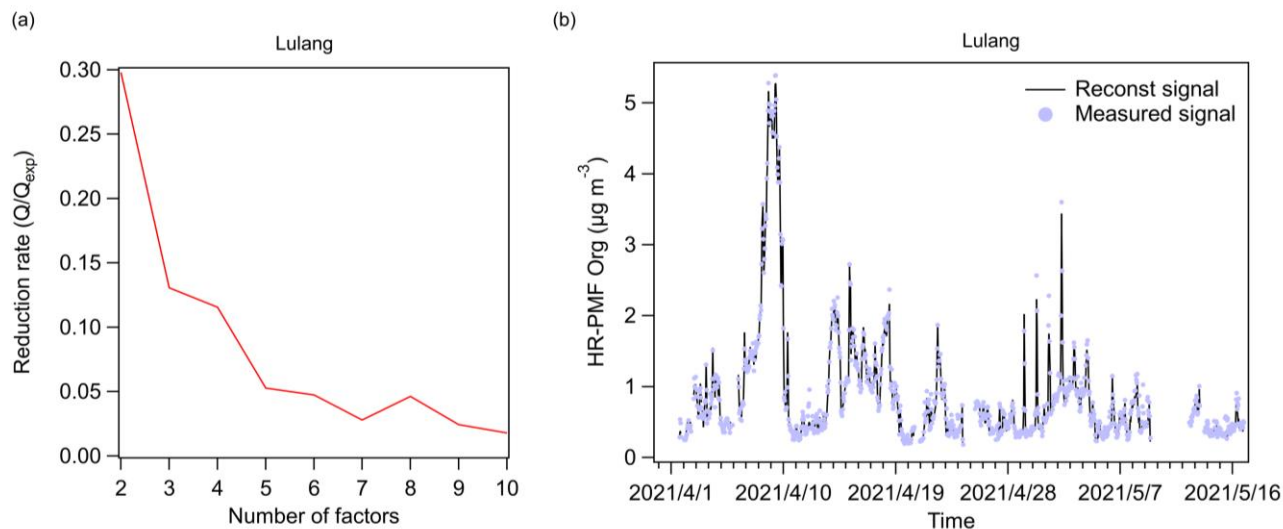


29

30

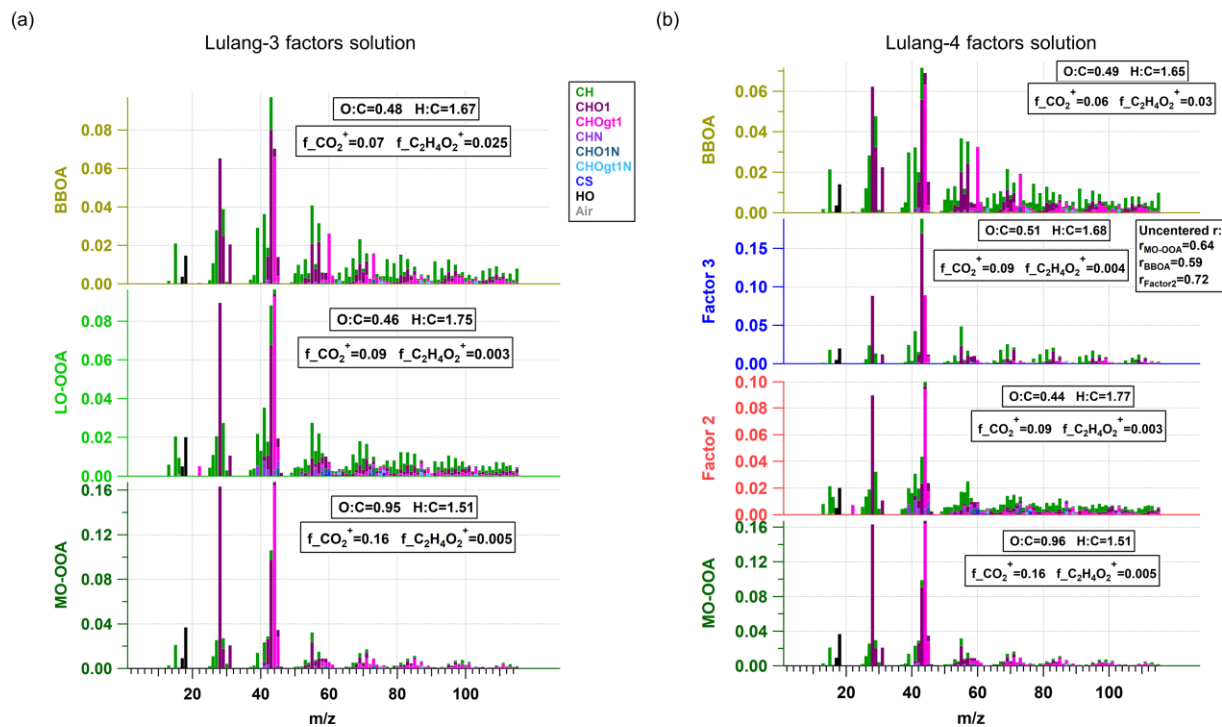
31

Figure S3: The time series of mass concentration of different organic aerosol factors identified by positive matrix factorization (PMF) in (a) Xihai and (b) Lulang.



33

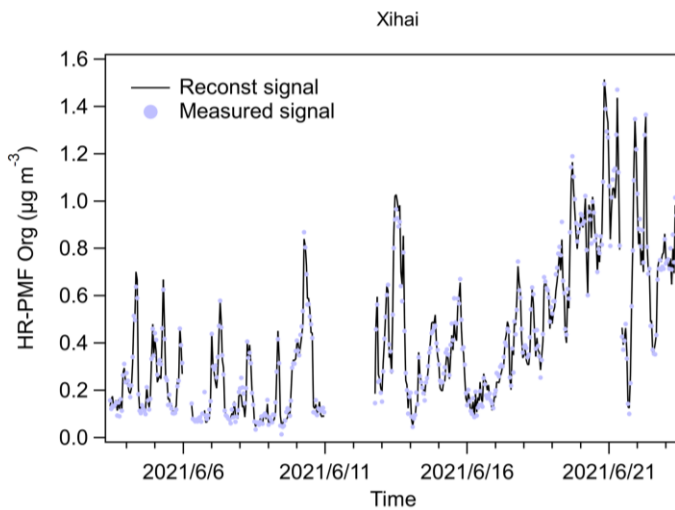
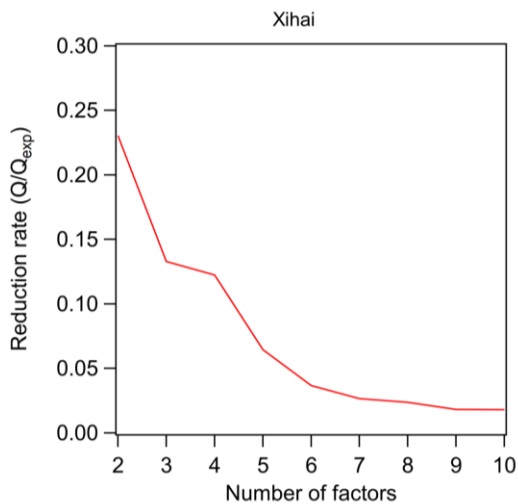
34 **Figure S4:(a) The variation of the reduction rate of  $Q/Q_{exp}$  with the number of factors in Lulang. (b) The time series of**  
 35 **reconstructed signal and measured signal for 3-factors solution.**



36

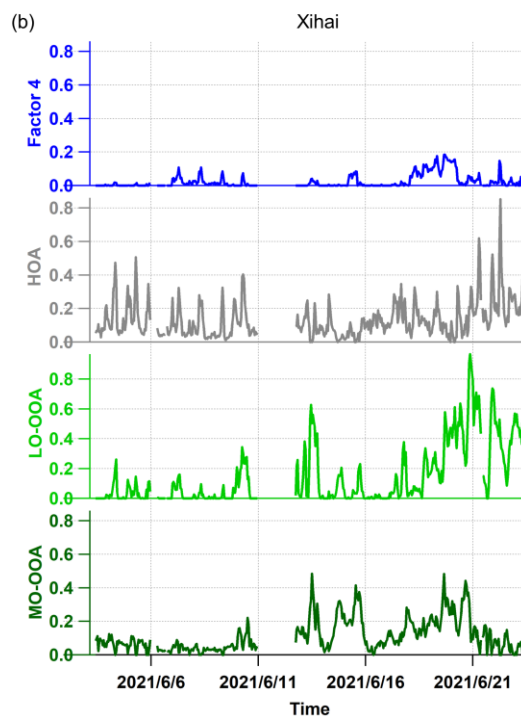
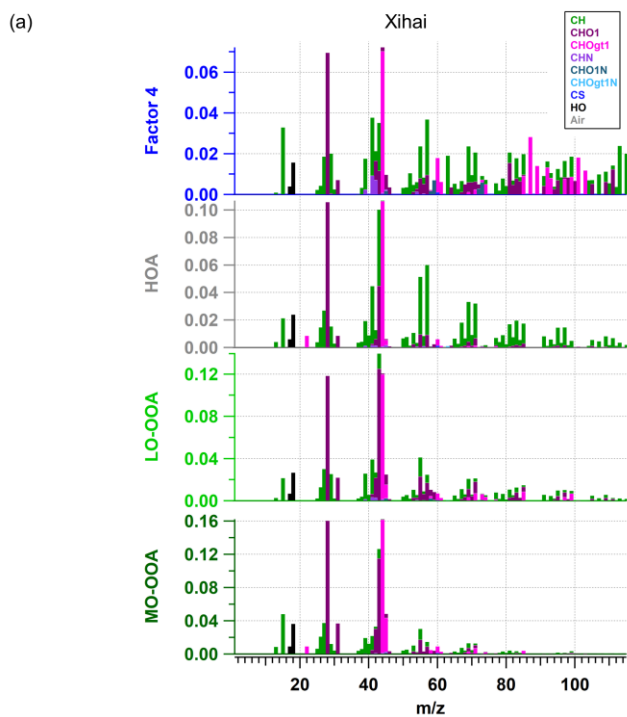
37

**Figure S5: The mass spectrum of factors in the (a) 3-factors solution and (b) 4-factors solution.**



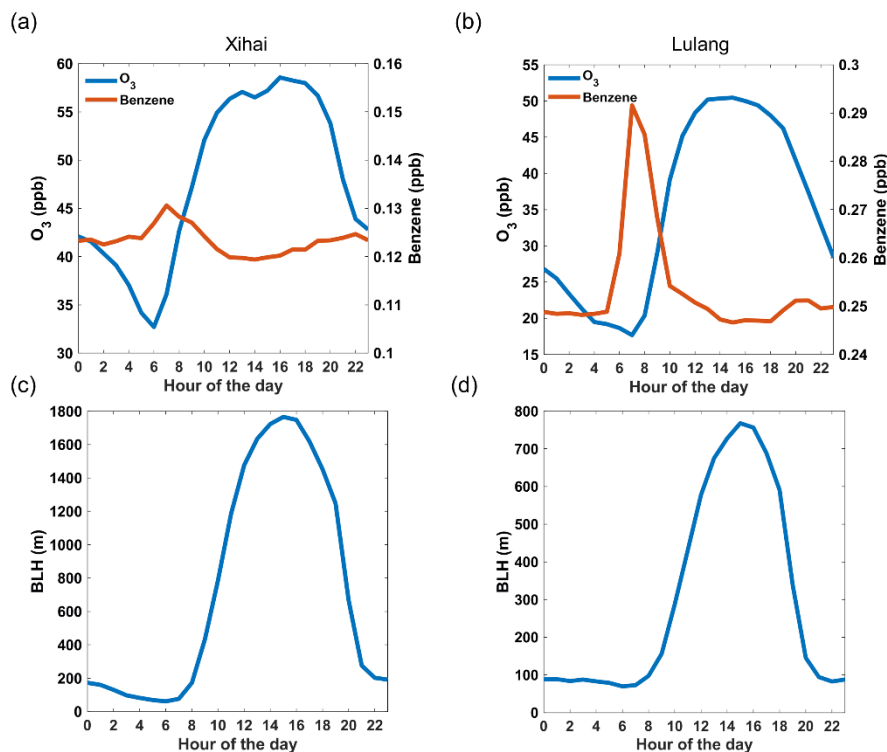
38

39 **Figure S6:**(a) The variation of the reduction rate of  $Q/Q_{exp}$  with the number of factors in Xihai. (b) The time series of  
40 reconstructed signal and measured signal for 3-factors solution.



41

42 **Figure S7:** The (a) mass spectrum and (b) time series of factors in the 4-factors solution.



44

45 **Figure S8: The diurnal variation of ozone (O<sub>3</sub>), benzene and boundary layer height (BLH) in Xihai (a,c) and Lulang (b,d).**

46 As the Fig. S8a shows, the O<sub>3</sub> and the benzene did not increase significantly after 15:00 (Beijing Time) in Xihai, indicating  
 47 that the secondary formation and pollutant emission were relatively stable without strong enhancement. In the afternoon, the  
 48 boundary layer height was also high in Xihai. It means that the atmospheric diffusion conditions were good but the PM<sub>BC</sub> in  
 49 the surrounding areas can be elevated from the surface to higher altitudes, facilitating pollutant transport. Summarily, not  
 50 secondary formation, emissions, rather pollutant transport caused that PM<sub>BC</sub> increased after 15:00 (Beijing Time) in Xihai.

## 51 References

52 Cappa, C. D., Zhang, X. L., Russell, L. M., Collier, S., Lee, A. K. Y., Chen, C. L., Betha, R., Chen, S. J., Liu, J., Price,  
 53 D. J., Sanchez, K. J., McMeeking, G. R., Williams, L. R., Onasch, T. B., Worsnop, D. R., Abbatt, J., and Zhang, Q.: Light  
 54 Absorption by Ambient Black and Brown Carbon and its Dependence on Black Carbon Coating State for Two California,  
 55 USA, Cities in Winter and Summer, *Journal of Geophysical Research-Atmospheres*, 124, 1550-1577,  
 56 10.1029/2018jd029501, 2019.

57 Chen, P. F., Kang, S. C., Li, C. L., Zhang, Q. G., Guo, J. M., Tripathee, L., Zhang, Y. A., Li, G., Gul, C., Cong, Z. Y.,  
 58 Wan, X., Niu, H. W., Panday, A. K., Rupakheti, M., and Ji, Z. M.: Carbonaceous aerosol characteristics on the Third Pole: A  
 59 primary study based on the Atmospheric Pollution and Cryospheric Change (APCC) network, *Environmental Pollution*, 253,  
 60 49-60, 10.1016/j.envpol.2019.06.112, 2019.



61 Mätzler, C.: MATLAB functions for Mie scattering and absorption, version 2, IAP Res. Rep [code], volume: 8,  
62 University of Bern, Bern, Switzerland, 2002.

63 Moosmüller, H., Chakrabarty, R. K., Ehlers, K. M., and Arnott, W. P.: Absorption Ångström coefficient, brown carbon,  
64 and aerosols: basic concepts, bulk matter, and spherical particles, Atmos. Chem. Phys., 11, 1217-1225, 10.5194/acp-11-  
65 1217-2011, 2011.